

# Physical–Chemical Characterization of Octreotide Encapsulated in Commercial Glucose-Star PLGA Microspheres

Avital Beig, Linglin Feng, Jennifer Walker, Rose Ackermann, Justin K. Y. Hong, Tinghui Li, Yan Wang, Bin Qin, and Steven P. Schwendeman\*

Cite This: *Mol. Pharmaceutics* 2020, 17, 4141–4151

Read Online

ACCESS |

Metrics & More

Article Recommendations

Supporting Information

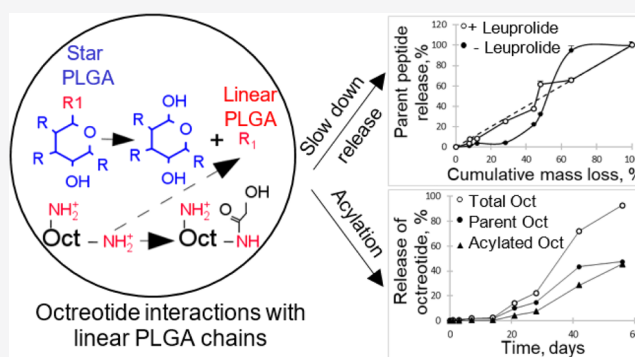
**ABSTRACT:** Sandostatin LAR (SLAR) is an injectable long-acting release (LAR) microsphere formulation for octreotide based on a biodegradable glucose star copolymer of D,L-lactic and glycolic acids (PLGA-glu), which is primarily used for the treatment of patients with acromegaly. There currently is no generic SLAR approved in the United States despite expiration of patent coverage. To understand better this important formulation, SLAR was assessed for its composition and physical–chemical properties. Octreotide release kinetics was monitored under physiological conditions over 56 days together with several bioerosion parameters [mass loss, water uptake, pH of release media, polymer molecular weight (Mw), and confocal microscopy after BODIPY uptake]. A significant increase in the amount of released peptide occurred after day 14. After 1 day of incubation in PBST, octreotide was not extractable completely from SLAR during 2 h of the extraction process, but complete extraction was accomplished after 24 h, which suggested that strong and noncovalent PLGA–octreotide interactions occurred beginning in the initial release phase. Leuprolide is considered as a cationic peptide competitor for octreotide–PLGA interactions and its presence in the release medium resulted in more continuous octreotide release from SLAR, which was linearly correlated with the mass loss from the polymer (*i.e.*, an indication of erosion-controlled release). These data strongly suggest that octreotide forms a salt with acid end groups of linear PLGA chains that are either present as impurities in, and/or produced by the degradation of, the PLGA-Glu. This salt is expected to catalyze octreotide acylation and extend peptide release beyond that driven by erosion control. The characterization studies of physicochemical properties of SLAR described here could be useful for the development and regulatory evaluation of generic octreotide microspheres as well as new polymer formulations, in which the polymer strongly interacts with encapsulated peptides.

**KEYWORDS:** biodegradable microspheres, controlled-release, peptide delivery, peptide–polymer interactions, PLGA

## 1. INTRODUCTION

Innovative technologies to create long-acting release formulations (LARs) are employed to improve treatment when the prolonged effect of the drug is required.<sup>1</sup> LAR drug products can attain steady therapeutic blood levels of molecules, such as peptides, for periods of weeks to months after a single injection or steady-state dosing.<sup>2</sup> Microencapsulation techniques are employed to extend biological half-life time, to reduce the frequency of injections, and to protect proteins and peptides from rapid degradation by enzymes.<sup>3</sup> Long-acting release formulations have a number of important advantages depending on the formulation such as high drug loading, sustained release of drug over time with little initial burst, and a small volume of injection.<sup>4</sup>

Sandostatin LAR (SLAR, Novartis Pharma AG) is a long-acting poly(lactic-co-glycolic acid) (PLGA)-based formulation of octreotide. It was designed for the treatment of patients with acromegaly and symptoms related to certain types of tumors.<sup>5</sup>



SLAR for intramuscular injection allows for the reduction in injection frequency from three times per day (subcutaneous solution formulation of octreotide) to once a month (long-acting release formulation).<sup>6</sup> There is currently no generic SLAR product approved in the United States. Measuring the SLAR composition and analyzing physicochemical characteristics of the product is important to assist companies pursuing generic products. Because SLAR contains one of the few peptides formulated as a microsphere product, it is also important to understand this formulation better when developing entirely new peptide/PLGA formulations. For

Received: June 11, 2020  
Revised: September 1, 2020  
Accepted: September 2, 2020  
Published: September 2, 2020



example, detailed information regarding SLAR can serve as an important commercial precedent when making decisions about the development and potential regulation of new depot formulations.

*In vitro* release testing of long-acting formulations when properly validated is very useful for relating formulation characteristics to pharmacokinetics and examining deviation in product quality. The release of encapsulated drug from PLGA-based microspheres can be affected by multiple factors: PLGA characteristics such as molecular weight, lactide-to-glycolide (L/G) ratio, star or linear chain branching, and end-group capping; drug and excipient loading; microencapsulation conditions, drying, and residual solvents; pH, temperature, and stir rate in release media; water uptake; and size, porosity, and shape of the microspheres.<sup>7</sup> Another difficulty associated with the employment of PLGA in designing formulations is related to the creation of acids during degradation, similar to other biodegradable polymers.<sup>7</sup>

In SLAR, a unique glucose star PLGA (PLGA-glu) is used to create a long-acting release formulation. SLAR is characterized by decreased bioavailability (60–63%) compared to the immediate release injection.<sup>8</sup> Previous *in vitro* release studies showed that octreotide becomes acylated in PLGA-glu microspheres.<sup>9</sup> An important goal of the current study was to examine stability of the octreotide as well as the nature of peptide–polymer interactions.<sup>10</sup>

## 2. EXPERIMENTAL SECTION

**2.1. Materials.** Octreotide acetate (purity >99.7%) was obtained from a GMP batch prepared by SHJNJ PHARMA-TECH INC., China. Sandostatin LAR (sterile 5 mL vials delivering 30 mg of octreotide free peptide, NDC Code 0078-0825-81) was purchased from the hospital pharmacy (University of Michigan hospital). Leuprolide acetate with purity >98% by HPLC analysis was purchased from Shanghai Soho-Yiming Pharmaceuticals Co. Ltd. (Shanghai, China). BODIPY FL (4,4-difluoro-5,7-dimethyl-4-bora-3a,4a-diaza-s-indacene-3-propionic acid) was purchased from Fisher Scientific. All solvents used were of HPLC grade and were purchased from Fisher Scientific, and unless otherwise noted, all other chemicals were purchased from Sigma-Aldrich.

**2.2. Determination of Octreotide Loading and Encapsulation Efficiency.** Octreotide loading was determined by two-phase extraction followed by UPLC. SLAR microspheres (~5 mg) were dissolved in 1 mL of methylene chloride. The mixture was vortexed for 2 min, and then 4 mL of acetate buffer (50 mM sodium acetate, pH = 4) was added. The resulting solution was vortexed for 2 or 24 h and analyzed for octreotide content by ultraperformance liquid chromatography (UPLC), as described below. Drug loading was calculated as the ratio of the mass of drug in the microspheres to the total mass of the microspheres. Note that SLAR microspheres in the final product contain mannitol on the surface, resulting in reduced drug loading relative to those microspheres after washing off mannitol.

SLAR microspheres were also analyzed for the nitrogen (N) content. Samples of microspheres (10 mg), octreotide (5 mg), and EDTA (0.5–2 mg) were weighed into a foil cup. The EDTA standard with a certified nitrogen content ( $9.57 \pm 0.03$ %) was supplied by LECO (St. Joseph, MI, USA). Samples of standards were run on a LECO model to detect total N. Before sample analysis, the system was calibrated with EDTA standards by analyzing blank and performing a drift correction.

Nitrogen was converted to peptide using a conversion factor, which was determined by analyzing pure octreotide.

**2.3. Octreotide Quantification by UPLC.** The amount of octreotide and its degradation products in the combined aqueous phase was determined using ultraperformance liquid chromatography (Acquity, Waters, Milford, MA, USA) equipped with an Acquity single quadrupole QDa mass detector (UPLC-MS), a UV detector set to 280 nm (UPLC), and a BEH C18 column 1.7  $\mu\text{m}$ , 2.1  $\times$  100 mm (Waters, Milford, MA, USA). A gradient elution using acetonitrile with 0.1% (v/v) formic acid and ddH<sub>2</sub>O with 0.1% formic acid at a flow rate of 0.5 mL/min was performed as follows: 0 min (25:75), 2 min (35:65), and 2.5 min (25:75) and a 0.5 min recovery. For quantitation of degradation products, the standard curve of the parent drug was used.

**2.4. Determination of the D-Mannitol Content.** Approximately 3 mg of each lot of SLAR products was taken out to 20 mL tubes. The formulation was dissolved with 10 mL of H<sub>2</sub>O and then sonicated with heating for 1 h. After filtration, the solutions were diluted with acetonitrile at 1:1 v/v ratio. The samples were injected into UPLC-MS (+ESI, 183.40 *m/z*) for the determination of the mannitol concentration [acetonitrile with 0.1% v/v formic acid and ddH<sub>2</sub>O with 0.1% formic acid (40:60) at a flow rate of 0.5 mL/min].

**2.5. Scanning Electron Microscopy.** Prior to imaging, microspheres were mounted onto aluminum specimen stubs by using double-sided carbon tape and coated with a thin layer of gold under vacuum. Scanning electron microscopy (SEM) was performed on a Tescan MIRA3 FEG scanning electron microscope. Images were captured by MiraTC software.

**2.6. Molecular Weight of PLGA.** The weight-averaged molecular weight (*M<sub>w</sub>*) of PLGA was measured by gel permeation chromatography (GPC). The Waters 1525 GPC system (Waters, USA) consisted of two styragel columns (HR 1 and HR 5-E columns), a binary HPLC pump, a waters 717 plus autosampler, a waters 2414 refractive index detector, and Breeze software to obtain the molecular weight. Samples were dissolved in tetrahydrofuran (THF) at a concentration of ~10 mg/mL and eluted with THF at 0.35 mL/min. The molecular weight of each sample was calculated using monodisperse polystyrene standards, *M<sub>w</sub>* 4130–107,000 Da.

**2.7. Determination of the Glass-Transition Temperature (*T<sub>g</sub>*).** SLAR microspheres (5 mg) were transferred to DSC aluminum pans, followed by sealing with hermetic lids. The dry *T<sub>g</sub>* was determined with a modulated differential scanning calorimeter (MDSC) (Discovery, TA Instruments, New Castle, DE) as previously reported.<sup>11</sup> Temperatures were ramped between –20 and 80 °C at 3°/min with a modulation amplitude of  $\pm 1^\circ$ /min. *T<sub>g</sub>* was taken as the midpoint of the reversing heat event. The results were analyzed by using TA TRIOS software, and all measurements were performed in triplicate for each sample.

**2.8. Determination of the Residual Solvent Content and Moisture Content.** The total residual solvent content was estimated by TGA and measured more specifically by GPC and Fischer titration, as described below. For TGA, 3–5 mg of microparticles was placed on a platinum pan and equilibrated at 25 °C and then ramped to 600 °C at 10 °C/min. The residual solvent content was estimated as the mass loss between 25 and 150 °C, which is much lower than the temperature range over which mass loss of the polymer occurs.<sup>12</sup>

The residual water content in microspheres was determined by Karl Fischer titration.<sup>13</sup> Samples (~0.1 mg each) were weighed into vials. Then, 0.1 mL of anhydrous dimethylsulfoxide (DMSO) was added to each sample to dissolve microspheres and the mixture was vortexed until complete dissolution. This solution (~0.1 g) was injected using a syringe in the reaction cell of a KF titrator. The stirring time in the cell before titration was fixed at 20 s. Five analyses were completed for each sample, and the respective results were averaged. The moisture content of the microspheres was determined after correction for the moisture level in the DMSO.

Residual solvents used in SLAR preparation were determined by GC. Samples (10 mg each) were weighed into glass vials. One mL of dimethyl sulfoxide was added. The glass vials were sealed immediately to prevent evaporation of methylene chloride (MC). The GC conditions were as follows: nitrogen gas was used as a carrier solvent at a flow rate of 25 mL/min, air flow was 350 mL/min, and hydrogen flow was 35 mL/min. The front detector temperature was 240 °C and the front inlet pressure was a constant flow at 2 mL/min. Each sample was agitated for 20 min at 80 °C. One milliliter of a headspace sample was injected into the front inlet with the temperature of 140 °C, a split flow of 40 mL/min, and a split ratio of 20. Column: TG-624 GC Column, 0.53 mm I.D., 30 m long, 3 μm film thickness. The GC column gradient was as follows: an initial temperature of 40 °C for 15 min, followed by an increase to 240 °C at 10 °C/min over 20 min and holding at 240 °C for 2 min. Residual solvents were identified by comparing their retention time with a retention time of standard solvents using an Agilent 7890B gas chromatograph (GC) combined with the Agilent 5977B MSD with MassHunter software. A 30 m long, 0.53 mm I.D. TG-624 GC column with a 3 μm film thickness was used. Helium was used as the carrier gas at a flow rate of 6.9 mL/min. The front inlet was set to 240 °C with a split flow of 10.0 mL/min and a split ratio of 10. The GC column gradient included an initial temperature of 40 °C for 15 min, followed by an increase to 230 °C at 10 °C/min over 20 min. Twenty milliliters of sample vials was agitated at 80 °C, and 1 mL of the headspace was injected.

**2.9. Determination of the Microsphere Size.** The size of the microspheres was determined by laser diffraction using a Malvern Mastersizer 2000, which provides a volume-weighted size distribution. Samples were added dropwise to ddH<sub>2</sub>O dispersant in the instrument until the desired obscuration level is reached (7–10% obscuration) at a constant stir speed of 2000 rpm. Measurements were conducted using a material refractive index of 1.59 and an absorbance of 0.01. A general-purpose calculation model, with normal calculation sensitivity and irregular particle shape, was selected for size calculations.

**2.10. Determination of the L/G Ratio by <sup>1</sup>H NMR.** To evaluate the LA/GA of the starting PLGA, 500 MHz <sup>1</sup>H NMR was used. Ten milligrams of SLAR was washed with water to remove the mannitol, and then the polymer was dissolved in chloroform at a concentration of 10 mg/mL. Chloroform was evaporated, and microspheres were dried in the vacuum oven at room temperature for 1 day. Before NMR analysis, microspheres were dissolved in chloroform. The pulse delay set was 18 s to ensure that all the spins were relaxed to the ground state.

**2.11. Measurement of Stability and Drug Release *in Vitro*.** Ten milligrams of SLAR microspheres was suspended in 1 mL of 10 mM phosphate-buffered saline (PBS) with 0.02%

sodium azide and 0.02% Tween 80 (PBST) at pH 7.4. Then, the microspheres were incubated at 37 °C with agitation at 80 rpm (KS 130 basic, IKA Works Inc., Wilmington, NC, USA), and after centrifugation at 4000g for 5 min, the entire medium was collected and replaced with 1 mL of the same buffer at days 1, 3, 7, 14, 21, 28, 42, and 56. To minimize particle loss during sampling, the supernatant was carefully removed using a fine tip pipette and if any visible microspheres were taken up, the supernatant was placed back in the tubes and the centrifugation/sampling was repeated. The amount of octreotide released to the release media was determined by UPLC. At each time point, octreotide was extracted by the two-phase extraction method and was analyzed for peptide stability and retention in the microspheres by UPLC.

**2.12. Examination of the Octreotide–Polymer Interactions by Competitive Binding to Leuprolide.** SLAR microspheres were placed in 1 mL of 4 mg/mL leuprolide solution in PBST in parallel with the release experiment. The microspheres were incubated at 37 °C with agitation at 80 rpm. After centrifugation (4000g for 5 min), the entire release media were collected, analyzed for the parent octreotide content by UPLC, and replaced with fresh leuprolide/PBST solution at days 1, 3, 7, 14, 21, 28, 42, and 56. Note that the leuprolide in the release media did not interfere with octreotide quantification but did prohibit the measurement of degradation products and the total peptide content.

**2.13. Quantification of Microsphere Water Uptake and Mass Loss.** Mass loss and water uptake were estimated as previously described.<sup>14</sup> Microspheres were incubated as in the release kinetic study and collected on preweighed nylon membrane filters under vacuum and washed off with ddH<sub>2</sub>O. Then, the surface water was removed by further filtration under vacuum for 5 s and the wet weight of the microspheres on the membrane was immediately measured. The samples on the nylon membrane were dried at room temperature under reduced pressure to a constant weight, and then the dry weight was recorded. To correct for the interparticle water, dry microspheres were suspended in PBST buffer solution (pH = 7.4) at 4 °C and the wet and dry weights of microspheres on the membrane were measured after filtering and drying. The weight difference between wet and dry particles was used to estimate the fraction of interparticle water ( $W_i$ ), as defined by

$$W_i = \frac{W'_1 - W'_2}{W'_2}$$

where  $W'_1$  and  $W'_2$  are the weights of wet and dry microspheres, respectively, after immediate collection at  $t = 0$ . The water uptake of microspheres at time  $t$  [ $W_p(t)$ ] was estimated by

$$W_p(t) = \frac{W_1 - W_2 - W_2 \times W_i}{W_2}$$

where  $W_1$  and  $W_2$  are the wet and dry microsphere weights after incubation at 37 °C in PBST buffer at time  $t$ . The percent mass loss was calculated according to the following equation

$$\% \text{ mass loss} = \frac{W_0 - W_3}{W_0} \times 100\%$$

where  $W_0$  is the initial weight of dry microspheres excluding the cryoprotectant and  $W_3$  is the weight of the microspheres after filtration and drying (subtracting the weight of the nylon membrane).

**2.14. BODIPY Uptake and Laser Scanning Confocal Microscopy.** SLAR microspheres were incubated as described in the release study. At days 1, 3, 7, 14, 21, 28, 42, and 56 during *in vitro* release, the release media were removed and replaced with fresh buffer at each time point. Before confocal microscopy analysis, microspheres at the time points above were incubated in a solution of BODIPY FL (5  $\mu\text{g}/\text{mL}$ ) in PBST buffer at 37 °C for 7 days under mild agitation. BODIPY distribution in degrading microspheres and subsequent image analysis was determined as previously described.<sup>15</sup> Microspheres were imaged using a Nikon A1 spectral confocal microscope (Nikon, Tokyo, Japan) to observe dye distribution and microsphere morphology. The excitation wavelength was set to 488 nm, and the detected emission wavelength was 525 nm (*i.e.*, the setting mode for FTIC analysis). The pinhole size was set on 1.2 AU, scan speed was 1.1 pixel dwell, and frame size was 512  $\times$  512. Images were acquired at 60 $\times$  magnification.

**2.15. Porosity.** A mercury intrusion porosimeter was used to determine the porosity of microparticles (AutoPore V Series, Micromeritics, Norcross, GA, USA). The penetrometer was loaded with 200–300 mg of microspheres (3cc powder penetrometer) to make the final stem volume 25–80%. The measurements were taken over low and high pressures varying from 0.5 psia to 61,000 psia (equilibration of 10 s at each pressure). The porosity was determined by the ratio between the intrusion volume and the bulk volume.

**2.16. Determination of the Acid Content.** The acid content was determined by organic phase titration.<sup>9</sup> First, PLGA was extracted from SLAR. Approximately 100 mg of particles was washed with cold ddH<sub>2</sub>O to remove mannitol and collected into a glass centrifuge tube, and then methylene chloride (1 mL) was added to dissolve microspheres. The mixture was vortexed for 30 min. After centrifugation at 4000g for 5 min, the entire media was collected and filtered through a 0.22  $\mu\text{m}$  PTFE syringe filter into a glass bottle. The bottle was left uncapped to allow methylene chloride to evaporate. After drying, the content was reconstituted in tetrahydrofuran/acetone 1:1 mixture (5 mL). Adding phenolphthalein methanol solution (0.1 wt %) as an indicator, the solution was immediately titrated with 0.01 M methanolic potassium hydroxide to a stable pink end point. The acid content of PLGA was calculated as follows

$$\text{acid content}[\text{mg KOH}/\text{g PLGA}] = \frac{(\text{volume of sample}[\text{mL}]) \times (N_{\text{NaOH}}) \times (M_{\text{wNaOH}})}{(\text{weight of PLGA}[\text{g}])}$$

### 3. RESULTS AND DISCUSSION

#### 3.1. Physicochemical Properties of Sandostatin LAR.

To characterize the stability and the amount of peptide in microspheres, the peptide was analyzed by UPLC after two-phase extraction and by nitrogen analysis. As shown in Table 1, octreotide loading in SLAR by both methods was close (4.57–4.76%) and comparable to the value listed in the package insert (4.6%). The particle size distribution of SLAR was narrow with a volume-median diameter of  $57 \pm 0.5 \mu\text{m}$  (mean  $\pm$  SEM,  $n = 3$ ) [ $d(v, 0.5)$ ]. Ten percent of the volume distribution was below  $34.4 \pm 0.2 \mu\text{m}$  (mean  $\pm$  SEM,  $n = 3$ ) [ $d(v, 0.1)$ ] and 90% of the volume distribution was below  $102.6 \pm 0.5 \mu\text{m}$  (mean  $\pm$  SEM,  $n = 3$ ) [ $d(v, 0.9)$ ]. These results were supported by the SEM micrographs. GPC analysis provided a

**Table 1. Characterization of Physical–Chemical Properties of SLAR**

property	measurement	measured value	expected value <sup>a</sup>
drug loading, %	extraction/UPLC N analysis	4.76 $\pm$ 0.11, 4.57 $\pm$ 0.08	4.65
mannitol content, %	UPLC	16.0 $\pm$ 0.5	17
moisture content, %	Karl Fischer titration	0.34 $\pm$ 0.08	N. R.
residual CH <sub>2</sub> Cl <sub>2</sub> , %	head space GC	0.12 $\pm$ 0.01	N. R.
residual heptane, %	head space GC	1.74 $\pm$ 0.03	N. R.
total residual solvent, %	TGA	2.11 $\pm$ 0.08	N. R.
Mw, kDa	GPC	46.5 $\pm$ 0.4	52.0 <sup>6,18</sup>
Mn, kDa	GPC	26.6 $\pm$ 0.4	N. R.
polydispersity	GPC	1.75 $\pm$ 0.02	N. R.
L/G ratio	<sup>1</sup> H NMR	55.3:44.7	55:45 <sup>6</sup>
porosity, %	Hg porosimetry	47	N. R.
size distribution	laser diffraction	$D(0.1)$ : 34.4, $D(0.5)$ : 57.8, $D(0.9)$ : 102.6	$D(0.1)$ : 20, $D(0.5)$ : 50, $D(0.9)$ : 100 <sup>6</sup>
$T_g$ , °C	DSC	45.64 $\pm$ 0.06	
acid value, $\mu\text{mol}/\text{g}$ polymer	titration	181	N. R.

<sup>a</sup>N.R. = not reported.

weight averaged of  $46.5 \pm 0.4$  kDa and a polydispersity of  $1.75 \pm 0.02$  for the PLGA in the product. The L/G ratio in the polymer was found to be 55.3:44.7 by <sup>1</sup>H NMR. Gas chromatography analysis revealed two residual solvents in SLAR: methylene chloride ( $0.12 \pm 0.01\%$ ) and heptane ( $1.74 \pm 0.03\%$ ), consistent with microencapsulation by coacervation.<sup>16,17</sup>

#### 3.2. Peptide–Polymer Interactions, Peptide Stability and Release, and Polymer Erosion Behavior under Physiological Conditions *in Vitro*.

It was previously shown that during encapsulation, storage, and release, octreotide interacts with linear PLGA acid end groups and acylation products are formed, primarily at the primary amino groups of the peptide.<sup>10</sup> To understand first whether peptide instability occurs in SLAR, we first conducted a long-term *in vitro* release study while monitoring for additional peptide species on the UPLC chromatogram. PLGA microspheres from SLAR were incubated in PBST (pH 7.4) at 37 °C over 56 days. As seen in Figure 1, SLAR microspheres exhibited a very low initial burst release over the first day before increasing gradually after the first 2 weeks. The low release during the first 2 weeks is consistent with the need of patients to remain on the immediate release formulation for the first 2 weeks of SLAR treatment.<sup>8</sup> From 2 to 4 weeks, a gradual but steady increase in release occurred before a very large release from 4 to 6 weeks. Then, there was a gradual tapering off by 6–8 weeks.

As the parent peptide began releasing during the active-release period, a large amount of octreotide degradation products was also observed in the release media (Figure 1). These products were similarly observed directly in the polymer matrix after the extraction of the peptide from microspheres (Figure 2). As shown in Figure 2, the degradation begins immediately after incubation as recorded by drops of the parent peptide and a growth of impurities in the first day extract. Calculations were made considering theoretical octreotide loading as 100%. The amount of total peptide

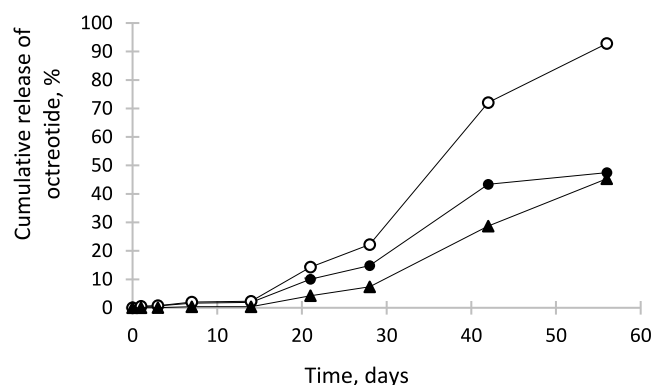


**Figure 1.** *In vitro* release kinetics of octreotide and its degradation products from SLAR microspheres determined in the release media. Microspheres were incubated in PBST pH 7.4 at 37 °C with mild agitation. The released peptide is depicted as parent octreotide (●), degradation products (▲), and total peptide (parent octreotide and degradation products) (○). Symbols represent mean ± S.E.M. ( $n = 3$ ).

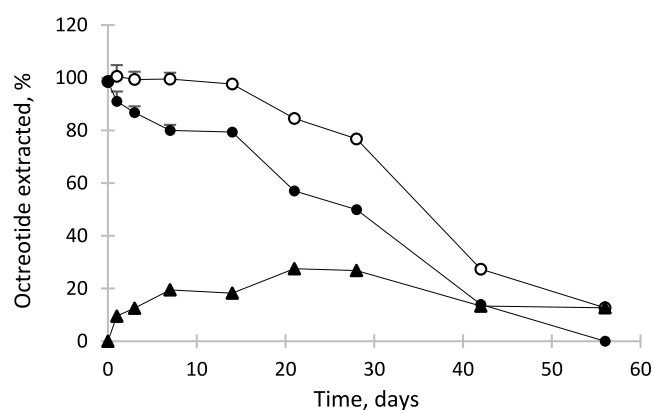


**Figure 2.** Octreotide and its degradation products extracted from SLAR microspheres during *in vitro* release. Microspheres were incubated in PBST pH 7.4 at 37 °C with mild agitation. The recovered peptide is depicted as parent octreotide (●), degradation products (▲) and total peptide (parent octreotide and degradation products) (○). The recovered peptide was normalized by the peptide content determined at time 0. Symbols represent mean ± S.E.M. ( $n = 3$ ).

extracted remained steady at around 100% of the peptide loading until day 14 and then began to decrease. This trend correlates with accelerated octreotide in release media after 14 days (Figure 1). To characterize the molecular weights of those additional peaks on the chromatogram, a MS detector was used. Figure 3 displays a representative LC–MS chromatogram of octreotide and degradation products extracted from microspheres after 7 days of incubation. The peak of octreotide appeared at 0.9 min and additional peaks were obtained in the spectrum at the later retention times.

As expected by the extensive literature of octreotide in linear PLGA systems, the peptide impurities were classified by LC–MS to be acylated adducts (*i.e.*, all molecular weights of the 15 peaks could be assigned as acyl additions by 1–3 lactic and glycolic units of the PLGA), presumed to occur primarily at the amino groups at the N-terminus and lysine side chain.<sup>10</sup> The masses of the acylation products recorded by the LC–MS detector are listed in Table S1. These peptide adducts were consistent with MW additions of a single lactic, single glycolic, sodium and lactic, two glycolic, and single lactic and single

glycolic acids. It is noted that in addition to the two expected more pronounced different sets (0.8–1.2 and 2–2.7 min) of peaks were identified as having glycolic and lactic acid additions attributable to the two primary amino groups of the peptide.<sup>10</sup> There was a third position (2.0–2.3 min) on the chromatogram, which may have been caused by one of the hydroxyl side chains of the peptide (*e.g.*, from thr-ol C-terminal amino acid residue).<sup>19</sup>

In Figure 4, we describe our hypothesis of how the peptide interacts with the PLGA polymer in SLAR and becomes acylated. Within the formulation, there exist both linear and star polymer chains with only the former possessing carboxylic acid end groups to form a salt with the cationic peptide. With time, new linear chains and new carboxylic groups are formed from every hydrolytic event on the parent star or linear polymer. Once the acetate counterion of the peptide is hydrated upon rapid water entry in the polymer, a fast proton transfer from linear PLGA carboxylic acid end groups is expected based on the higher pKa of acetic acid and the electron-withdrawing ester adjacent to the PLGA acid end group.<sup>21</sup> At the same time, the permanently cationic peptide will reasonably associate with the new anionic sites of the polymer. As we have learned recently, octreotide when forming such a salt can enter the polymer phase of low molecular weight linear acid-capped PLGAs.<sup>22</sup> The much more stable leuprolide is also capable of this salt formation-polymer phase entry,<sup>22</sup> which has been previously linked to several desirable effects such as increased encapsulation efficiency by the solvent evaporation and a higher  $T_g$  in the polymer.<sup>23,24</sup> This peptide absorption means that the peptide will become in very close proximity to either another region of the polymer chain or in fact other polymer chains within the polymer phase. As such, the second primary amino group (either deprotonated in the polymer phase or associated with a second PLGA-carboxylate chain) is free to attack the intact ester bond of PLGA (in the latter case upon proton exchange with hydronium ion or newly formed carboxylic acid from the polymer). The unstable tetrahedral intermediate will then lose water to liberate the acylated peptide and smaller linear PLGA chain.

As seen below, the peptide–PLGA interactions may also play an important role in octreotide release from SLAR. With the beginning of the active release phase, the amount of acylated products proceeded continuously until the end of the incubation. The two-phase extraction method used to estimate the octreotide content in microspheres normally included 2 h of vortexing to extract peptide from the organic layer to the water layer. This method allows extraction of 100% of octreotide from SLAR microspheres at time 0. After 1 day of incubation, the total peptide released was only 0.5% (Figure 5A), although the amount of total octreotide extracted by the two-hour extraction method reached only 89% (Figure 5B). By extension of the extraction time up to 24 h, it was possible to extract around 100% of total peptide after 1 day of incubation. The longer two-phase extraction method was used for the rest of the release study. Failure to extract the peptide completely after 1 day of incubation using the same extraction method as was used for time 0 suggests significant interactions between the peptide and the polymer. Note that the star polymer in SLAR contains significant acid (acid content 181  $\mu\text{mol acid}/1\text{ g polymer}$ , Table 1), which indicates the presence of significant linear chains and/or free monomers in this polymer. As glucose hydroxyls form the ester-capped ends of the PLGA chains in the star polymer, there is no conceivable way for

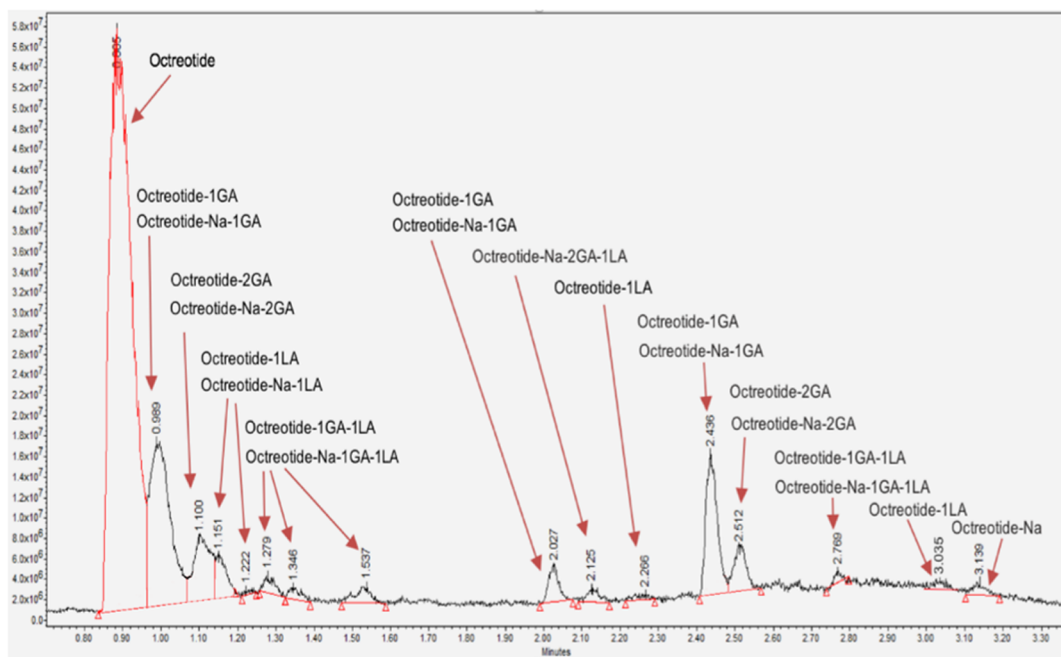


**Figure 3.** Total ion current plot identifying parent peptide and acylation sites of octreotide extracted from SLAR microspheres incubated 28 days in PBST pH 7.4 at 37 °C. Peaks were identified separately by mass.

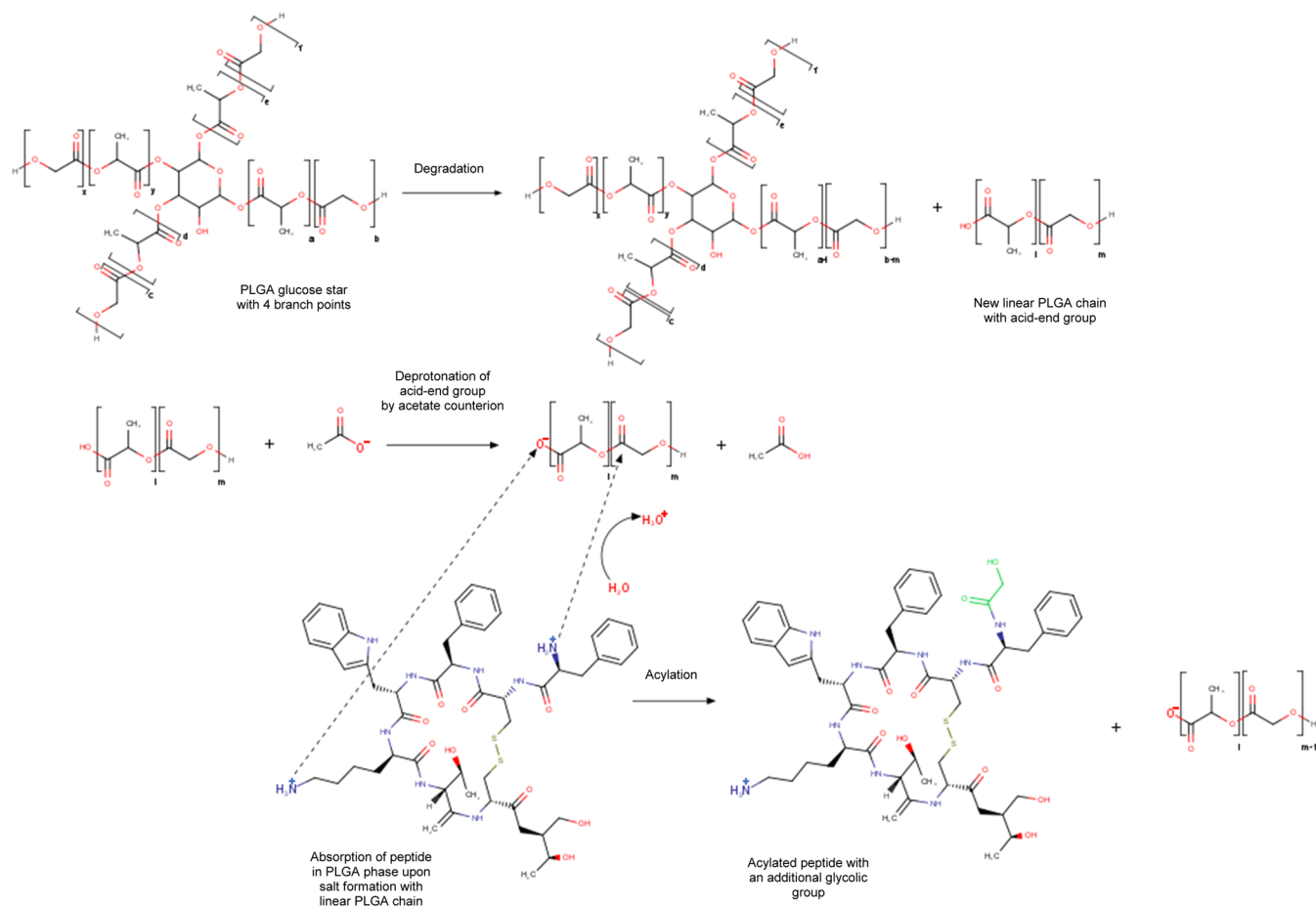


**Figure 4.** Proposed mechanism of octreotide acylation by PLGA-Glu star based on refs 10 and 20.

acids to be present in the polymer chain unless the acid originates from a linear polymer chain. It is possible that some of the acid measured in the polymer could be from acetic acid

(max acetate in SLAR = 117  $\mu\text{mol acid/1 g polymer}$  for the upper limit of 1.4–2.5 acetate/octreotide mol equivalent specification<sup>25</sup>) from the reaction of the acetate peptide

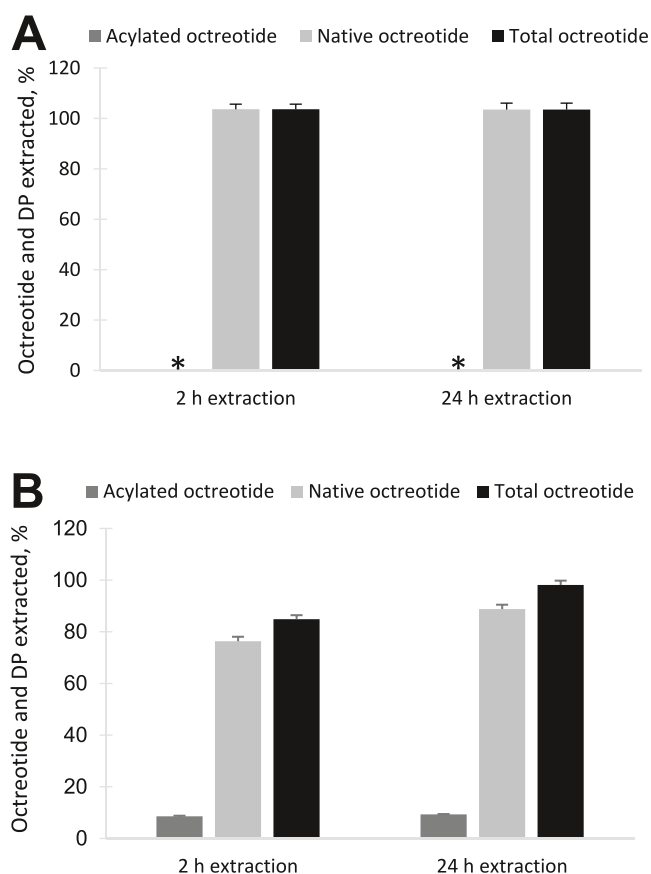


**Figure 5.** Recovery of octreotide extracted from SLAR by UPLC as a function of time of extraction (2 or 24 h) using microspheres without incubation (A) or after 24 h of incubation in PBST pH 7.4 at 37 °C (B) (normalized by octreotide loading at time 0). \* No acylated peptide was detected before incubation. Data represent mean  $\pm$  SEM,  $n = 3$ .

counterion with the more acidic acid of a linear PLGA chain.<sup>21</sup> Because the 24 h extraction allowed complete extraction of the peptide, it is reasonable to speculate that either the salt between octreotide and linear PLGA chains (or less likely other noncovalent bonds between the peptide and the polymer) were broken. The result of recovering all the peptide in a nonacylated form confirms the likelihood that the initial peptide–polymer interactions present in the SLAR microspheres are noncovalent. However, the possibility of some hydrolysis of covalent peptide–polymer attachments cannot be ruled out, which would require hydrolysis of a covalent bond during the extended extraction period. In Figure 6, the kinetics of the mass balance between increase in total peptide released and decline in total peptide extracted is displayed. It can be seen that the total of octreotide extracted and released was close to 100% at every time point supporting the completeness of peptide extraction and the independence of the extinction coefficient of peptide impurities at the detection wavelength (280 nm).

Polymer degradation plays a key role in the polymer erosion and release of drugs. To study the Mw kinetics, SLAR microspheres were incubated in PBST (pH 7.4) at 37 °C (the same conditions as were applied in the release study). Mw was examined at the same time points when the samples were subjected to release analysis. After 14 days of release, Mw of the polymer approached a very low level (<17 kDa) (Figure

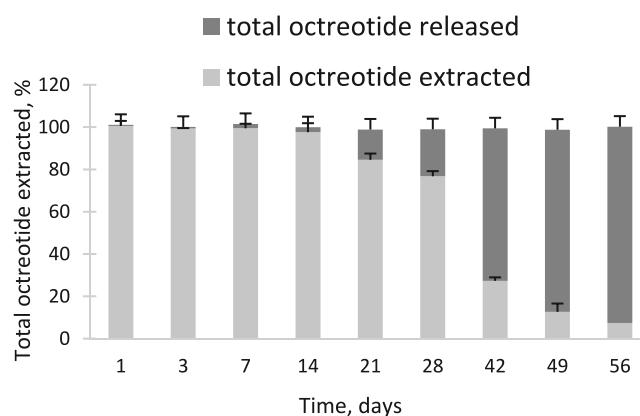


**Figure 6.** Mass balance of total peptide released (dark gray) and extracted (light gray) during *in vitro* release evaluation of SLAR microspheres. Data represent mean  $\pm$  SEM,  $n = 3$ .

7A) and the active release phase began. Beyond this time point, the polymer degradation rate sharply increased, followed by enhanced release of octreotide into the release media.

The physical–chemical behavior of PLGA is well described in the pharmaceutical literature.<sup>24,25</sup> The change in polymer chain geometry in the form of a glucose-centered star gives rise to increased water uptake and increased polymer chain mobility.<sup>20–22</sup> Degradation of the polymer occurs after its rapid hydration.<sup>30</sup> It is important to estimate the water uptake by PLGA microspheres in order to study the erosion behavior and potential influence on drug release and stability. Hydrolysis of the polymer is dominated by water in the polymer phase and release is sometimes triggered by changes in osmotic pressure inside the pores of the microspheres. The water uptake was calculated and corrected for estimated interparticle water when dry microspheres were suspended in cold buffer and immediately filtered, and the weight of wet and dry microspheres on the membrane was measured. After day 14, the water uptake exceeded 15% and started to increase dramatically reaching 50% by day 28 (Figure 7B). These data correlate with the beginning of the active phase of release and can be explained by increasing the pore size during degradation of the polymer.<sup>26–29</sup>

Mass loss was measured in order to study the potential release mechanism of erosion. Degradation of the polymer enhances the pore size of the microspheres by creation of osmotically active low molecular weight monomers and oligomers, which are slowly liberated into the release media. Increased pore size of the microspheres causes release of peptide molecules into release buffer from the polymer matrix. Under ideal erosion control, this liberation of peptides is expected to happen at a similar rate as polymer erosion. Mass loss of SLAR microspheres increased after day 7 of release, which is correlated with molecular weight decline and water uptake increase after 1 week (Figure 7C). Figure 8 illustrates a relationship between mass loss and release. The release rate was initially slower than the rate of erosion (*i.e.*, data falling below the release = erosion line). This unexpected effect can be explained by the healing of newly created pores during degradation of the polymer before the peptide has had a chance to desorb from the polymer.<sup>11</sup> See later discussion with leuprolide as the inhibitor of peptide–polymer interactions.

Octreotide–polymer interactions were also examined by competitive binding to leuprolide. Previously, our group

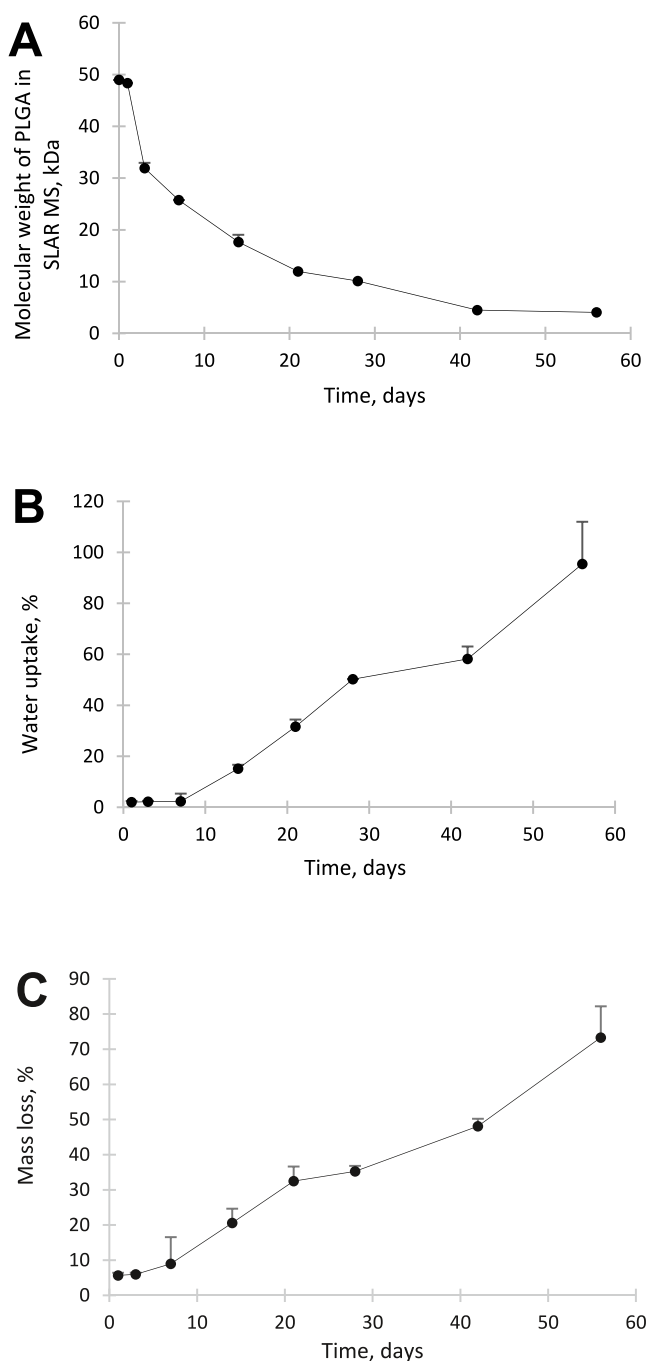


**Figure 7.** Kinetics of erosion behavior of SLAR in PBST pH 7.4 at 37 °C, including (A) Mw decline, (B) water uptake, and (C) mass loss. Symbols represent mean  $\pm$  S.E.M ( $n = 3$ ).

demonstrated that octreotide and leuprolide bind to low molecular weight linear acid-capped PLGA with a similar binding constant and stoichiometry.<sup>22</sup> Ester-capped PLGA binding to octreotide is expected to increase after degradation of the polymer, which causes steadily more acid end groups.<sup>10</sup> However, if acid-terminated linear chains are present initially, then one could expect peptide–PLGA interactions even at early time points. For example, a significant level of acid (acid number 181  $\mu\text{mol}/1 \text{ g}$  polymer, Table 1) was observed, as described before, indicative of the presence of linear PLGA chains in the formulation. We studied the release of octreotide in a modest concentration of leuprolide (4 mg/mL in PBST

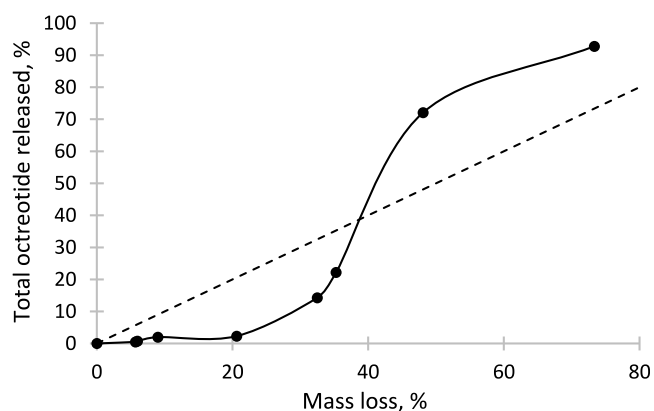


**Figure 8.** Relationship between cumulative release of total octreotide and mass loss of SLAR incubated in PBST pH 7.4 at 37 °C. Dotted lines indicate an ideal erosion-mediated release,  $y = x$ , as a reference. Symbols represent mean  $\pm$  S.E.M ( $n = 3$ ).

pH 7.4) to examine the effect of octreotide binding to the polymer on octreotide release. At every time point, the release medium was replaced by fresh leuprolide solution and analyzed for octreotide content by UPLC. We observed that octreotide was released initially much faster (Figure 9), consistent with

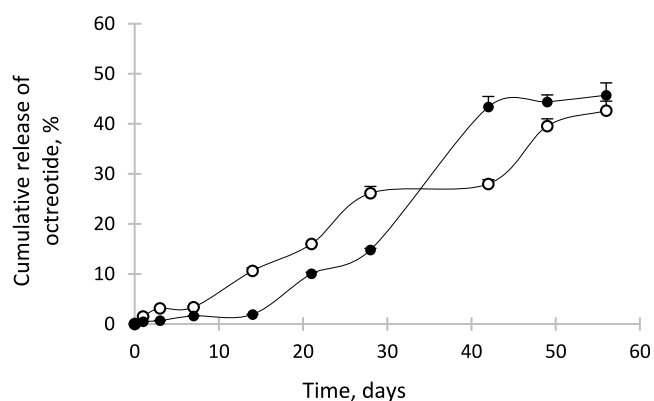


**Figure 9.** Cumulative release of native octreotide during incubation in PBST pH 7.4 at 37 °C in the presence (○) or absence (●) of 4 mg/mL adsorption competitor leuprolide. Symbols represent mean  $\pm$  S.E.M ( $n = 3$ ).

the hypothesis that noncovalently octreotide bound to star polymer was easily displaced by the PLGA-binding competitor, leuprolide. The release of octreotides in the presence of leuprolide was continuous and increased rapidly after 7 days of incubation. A reasonable explanation for this difference was not only PLGA–peptide interactions but also that pores are known to close spontaneously owing to polymer healing.<sup>15</sup> Thus, if the peptide is bound to the PLGA, then the time scale of opening of percolating pore networks before pore closure may be too short during early stages of release. In support of this hypothesis, we plotted the drug release *versus* mass loss kinetics, as shown in Figure 10, but this time both in the presence and absence of leuprolide. Note that because the presence of leuprolide in the release media interfered with acylated peaks of octreotide, the release of the parent peptide was plotted after normalization for the release of the parent drug after day 56. Mass loss was similarly normalized by the value at day 56. As expected from the similar kinetics of parent and total peptide (Figure 1), the leuprolide-free release-mass

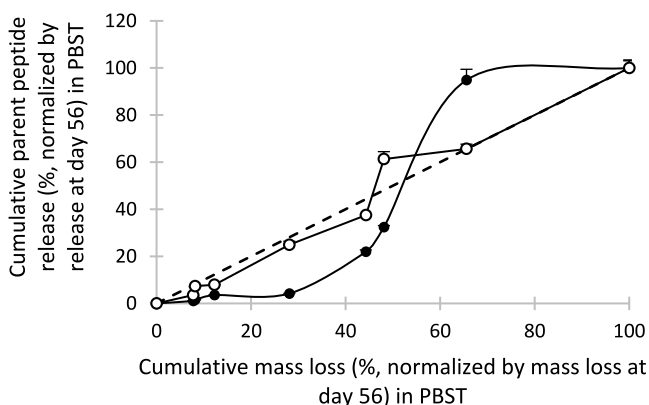


**Figure 10.** Relationship between cumulative release of the parent octreotide (normalized by release at day 56) in the presence (○) or absence (●) of 4 mg/mL adsorption competitor leuprolide and mass loss (normalized by mass loss at day 56) of SLAR incubated in PBST pH 7.4 at 37 °C. Dotted lines indicate an ideal erosion-mediated release,  $y = x$ , as a reference. Symbols represent mean  $\pm$  S.E.M ( $n = 3$ ).

loss curve (Figure 10) was very similarly s-shaped as was observed in Figure 8, owing to the strong interaction of octreotide with linear PLGA chains inhibiting peptide release. However, when the release of octreotide in the leuprolide-containing media was plotted *versus* mass loss (Figure 10), strikingly an ideal erosion behavior was observed (*i.e.*, release roughly equals mass loss). In other words, these data are consistent with the idea that when leuprolide is present, the peptide–polymer interaction effect on release is nullified and the release kinetics of octreotide defaults to the mass loss (erosion control) mechanism. Therefore, the peptide–polymer interactions appear to play a role in not only peptide acylation but also peptide release from SLAR.

To understand how the above release behavior was tied to changes in the polymer, the evolution of porosity of the polymer matrix was first characterized following BODIPY uptake by using confocal imaging (Figure 11). During the release study, the samples were taken out at each time point,

dried, and incubated for 3 days with BODIPY dye at 37 °C. BODIPY dye diffused throughout the microspheres<sup>15</sup> and was observed by laser fluorescence confocal microscopy. Green regions of strongly partitioned BODIPY in the images designate polymer microstructure deep within the polymer matrix owing to the dyes favorable PLGA partitioning. Black spots represent aqueous pores and pore interconnections in the particle. After 7 days of release study and 3 days of incubation in BODIPY, the inner pores of microspheres become larger. After 14 days of release, these pores start to interconnect with one another and thus break through the polymer matrix. This provides strong evidence of an important osmotic role in octreotide release from the SLAR. Also shown in these images is the tendency of polymer healing, as indicated by few interconnected pores on the surface of the microspheres.<sup>11,31</sup> Note that from separate studies of annealing in-house octreotide-loaded glucose star PLGA formulations, we observe that the glucose polymer appears to heal pores faster than either ester end-capped or acid-capped PLGAs.<sup>32</sup>

The external morphology of SLAR microspheres during the release study was also monitored by SEM. Pores appeared on the surface, shown at magnifications 9, 4.6, 2.7 kx (Figures 12 and S1 and S2). The pores were small until day 3 of incubation. At day 7, the surface of microspheres started changing. Large pores appeared at day 14 and the porosity increased drastically. After 1 month, release channels formed between pores and osmotic breakage pores were also evident in these electron micrographs. After day 42, it was impossible to find separate microspheres as the microspheres were broken and stuck together. These images clearly indicate that 2 weeks was a critical time point for the release of octreotide from PLGA microspheres, before which the polymer matrix was too nonporous for peptide release, consistent with the release and mass loss lag phase (Figures 12 and S1 and S2).

#### 4. SUMMARY

As formulators and FDA seek to understand the important distinguishing characteristics of SLAR, the findings described above bring additional clarity to this formulation and are significant in several ways, namely: (a) reverse engineering of

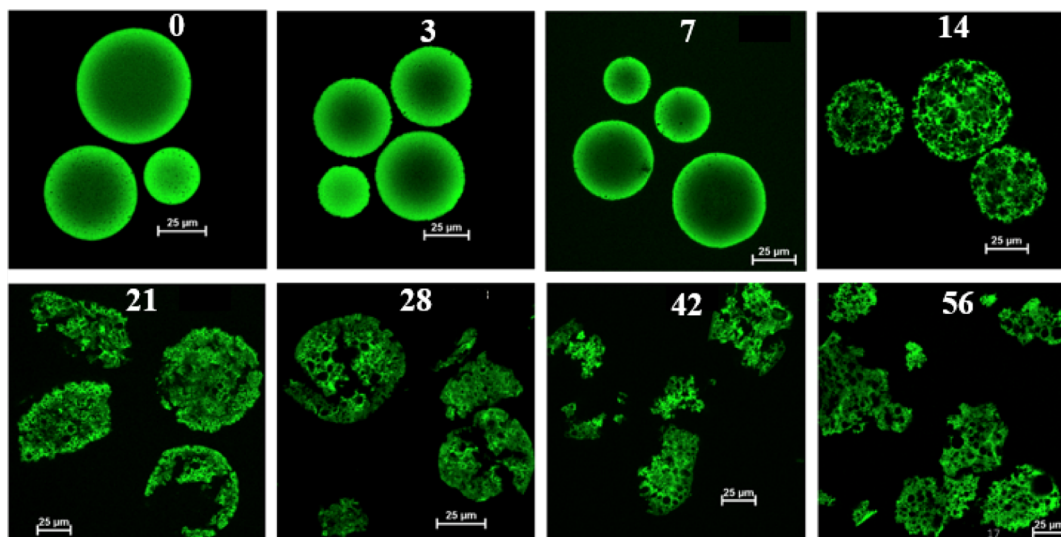


**Figure 11.** Confocal microscopy images of octreotide-loaded PLGA microspheres incubated in release media PBST pH 7.4 at the designated times (noted in each panel) and then further incubating with 5  $\mu$ g/mL BODIPY dye in the same media for 3 days.

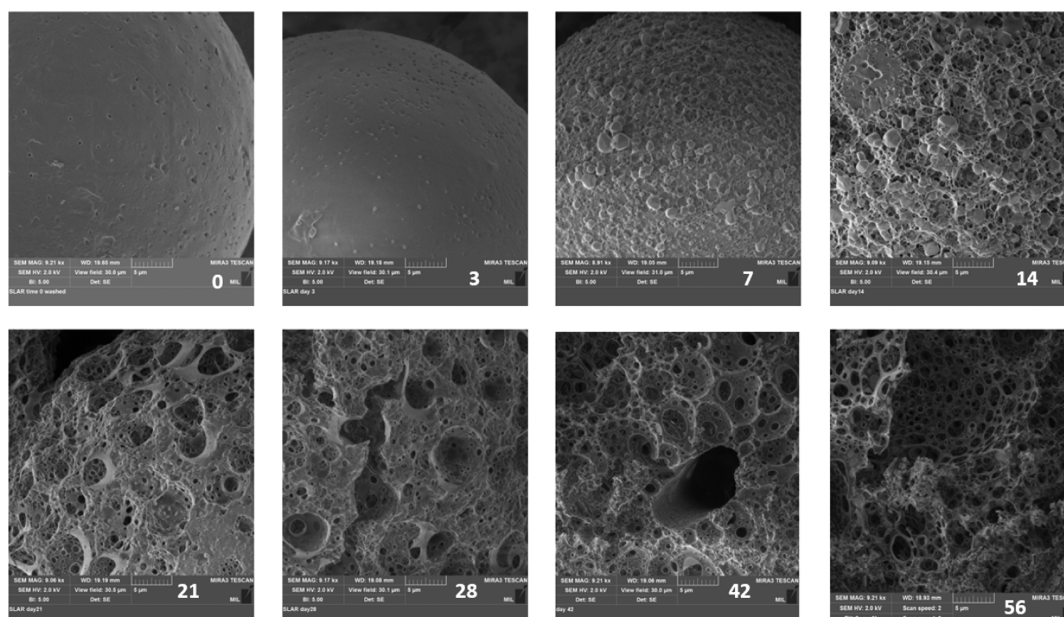


**Figure 12.** Scanning electron micrographs of SLAR microspheres incubated in PBST pH 7.4 over 56 days. Numbers in figures refer to days of incubation. Magnification was 9kx.

the novel LAR was conducted with a full list of assays, product composition, and quantitative attributes; (b) methods for quantitative extraction of octreotide from the polymer were developed that are not compromised by peptide–polymer interactions; (c) the broad distribution of encapsulated octreotide adducts recovered from the glucose star polymer during *in vitro* release were identified by UPLC/MS; (d) degradation and release kinetics was quantified with full mass balance, providing a plausible explanation for the reduced bioavailability of the LAR in humans relative to the soluble injected drug; (e) imaging of the unique microspheres was accomplished in dry and wet states by scanning electron and confocal imaging showing the clear effects of swelling on the development of interconnected pore networks; and (f) the key role of polymer–peptide interactions on peptide release, reasonably expected between octreotide and linear PLGA chains, which was even slower than the mass loss of the polymer; this interaction was implicated by release experiments in the presence and absence of a peptide inhibitor for octreotide–PLGA interactions. These findings may also be useful for analysis of future PLGA depots for other peptides and proteins.

## ■ ASSOCIATED CONTENT

### Supporting Information

The Supporting Information is available free of charge at <https://pubs.acs.org/doi/10.1021/acs.molpharmaceut.0c00619>.

Retention time and mass balance of octreotide and its degradation products and scanning electron micrographs of SLAR microspheres incubated in PBST pH 7.4 (PDF)

## ■ AUTHOR INFORMATION

### Corresponding Author

**Steven P. Schwendeman** – Department of Pharmaceutical Sciences and the Biointerfaces Institute and Department of Biomedical Engineering, University of Michigan, Ann Arbor,

Michigan 48109, United States; [orcid.org/0000-0003-3470-624X](https://orcid.org/0000-0003-3470-624X); Phone: 734/615-6574; Email: [schwende@umich.edu](mailto:schwende@umich.edu)

## Authors

**Avital Beig** – Department of Pharmaceutical Sciences and the Biointerfaces Institute, University of Michigan, Ann Arbor, Michigan 48109, United States

**Linglin Feng** – Department of Pharmaceutical Sciences and the Biointerfaces Institute, University of Michigan, Ann Arbor, Michigan 48109, United States

**Jennifer Walker** – Department of Pharmaceutical Sciences and the Biointerfaces Institute, University of Michigan, Ann Arbor, Michigan 48109, United States

**Rose Ackermann** – Department of Pharmaceutical Sciences and the Biointerfaces Institute, University of Michigan, Ann Arbor, Michigan 48109, United States

**Justin K. Y. Hong** – Department of Pharmaceutical Sciences and the Biointerfaces Institute, University of Michigan, Ann Arbor, Michigan 48109, United States; [orcid.org/0000-0003-0403-6679](https://orcid.org/0000-0003-0403-6679)

**Tinghui Li** – Department of Pharmaceutical Sciences and the Biointerfaces Institute, University of Michigan, Ann Arbor, Michigan 48109, United States

**Yan Wang** – Office of Research and Standards, Office of Generic Drugs, Center for Drug Evaluation and Research, U.S. Food and Drug Administration, Silver Spring, Massachusetts 20993, United States

**Bin Qin** – Office of Research and Standards, Office of Generic Drugs, Center for Drug Evaluation and Research, U.S. Food and Drug Administration, Silver Spring, Massachusetts 20993, United States

Complete contact information is available at:

<https://pubs.acs.org/doi/10.1021/acs.molpharmaceut.0c00619>

## Notes

The authors declare no competing financial interest.

## ACKNOWLEDGMENTS

This research was funded by FDA grant U01 FD005847. This paper reflects the views of the authors and should not be construed to represent the FDA's views or policies.

## REFERENCES

- (1) Schwendeman, S. P. Recent Advances in the Stabilization of Proteins Encapsulated in Injectable PLGA Delivery Systems. *Crit. Rev. Ther. Drug Carrier Syst.* **2002**, *19*, 73–98.
- (2) Wischke, C.; Schwendeman, S. P. Principles of Encapsulating Hydrophobic Drugs in PLA/PLGA Microparticles. *Int. J. Pharm.* **2008**, *364*, 298–327.
- (3) Ma, G. Microencapsulation of Protein Drugs for Drug Delivery: Strategy, Preparation, and Applications. *J. Controlled Release* **2014**, *193*, 324–340.
- (4) Crotts, G.; Park, T. G. Protein Delivery from Poly(Lactic-Co-Glycolic Acid) Biodegradable Microspheres: Release Kinetics and Stability Issues. *J. Microencapsul.* **1998**, *15*, 699–713.
- (5) Colao, A.; Merola, B.; Ferone, D.; Lombardi, G. Acromegaly. *J. Clin. Endocrinol. Metab.* **1997**, *82*, 2777–2781.
- (6) Grass, P.; Marbach, P.; Bruns, C.; Lancranjan, I. Sandostatin LAR (microencapsulated octreotide acetate) in acromegaly: Pharmacokinetic and pharmacodynamic relationships. *Metabolism* **1996**, *45*, 27–30.
- (7) Fredenberg, S.; Wahlgren, M.; Reslow, M.; Axelsson, A. The mechanisms of drug release in poly(lactic-co-glycolic acid)-based drug delivery systems-A review. *Int. J. Pharm.* **2011**, *415*, 34–52.
- (8) Sandostatin, L. Depot [Package Insert]; Novartis Pharmaceuticals Corporation: East Hanover, NJ, 2011.
- (9) Zhang, Y.; Sophocleous, A. M.; Schwendeman, S. P. Inhibition of Peptide Acylation in PLGA Microspheres with Water-Soluble Divalent Cationic Salts. *Pharm. Res.* **2009**, *26*, 1986–1994.
- (10) Na, D. H.; DeLuca, P. P. PEGylation of Octreotide: I. Separation of Positional Isomers and Stability Against Acylation by Poly(D,L-Lactide-co-Glycolide). *Pharm. Res.* **2005**, *22*, 736–742.
- (11) Mazzara, J. M.; Balagna, M. A.; Thouless, M. D.; Schwendeman, S. P. Healing Kinetics of Microneedle-Formed Pores in PLGA Films. *J. Controlled Release* **2013**, *171*, 172–177.
- (12) Kim, J.; Hong, D.; Chung, Y.; Sah, H. Ammonolysis-Induced Solvent Removal: A Facile Approach for Solidifying Emulsion Droplets into PLGA Microspheres. *Biomacromolecules* **2007**, *8*, 3900–3907.
- (13) Costantino, H. R.; Langer, R.; Klibanov, A. M. Moisture-Induced Aggregation of Lyophilized Insulin. *Pharm. Res.* **1994**, *11*, 21–29.
- (14) Liu, Y.; Schwendeman, S. P. Mapping Microclimate pH Distribution inside Protein-Encapsulated PLGA Microspheres Using Confocal Laser Scanning Microscopy. *Mol. Pharm.* **2012**, *9*, 1342–1350.
- (15) Kang, J.; Schwendeman, S. P. Determination of Diffusion Coefficient of a Small Hydrophobic Probe in Poly(Lactide-Co-Glycolide) Microparticles by Laser Scanning Confocal Microscopy. *Macromolecules* **2003**, *36*, 1324–1330.
- (16) Albayrak, C. Induced Phase Transition Method for the Production of Microparticles Containing Hydrophobic Active Agents. U.S. Patent 6,899,898 B2, 2005.
- (17) Bodmer, D.; Fong, J. W.; Kissel, T.; Maulding, H. V.; Nagele, O.; Pearson, J. E. Sustained Release Formulations of Water Soluble Peptides. U.S. Patent 5,639,480 A, 1997.
- (18) Petersen, H.; Bizec, J.-C.; Schuetz, H.; Delporte, M.-L. Pharmacokinetic and technical comparison of Sandostatin LAR and other formulations of long-acting octreotide. *BMC Res. Notes* **2011**, *4*, 344.
- (19) Shirangi, M.; Hennink, W. E.; Somsen, G. W.; van Nostrum, C. F. Identification and Assessment of Octreotide Acylation in Polyester Microspheres by LC-MS/MS. *Pharm. Res.* **2015**, *32*, 3044–3054.
- (20) Rastogi, S.; Kurelec, L.; Lemstra, P. J. Chain Mobility in Polymer Systems: On the Borderline between Solid and Melt. 2. Crystal Size Influence in Phase Transition and Sintering of Ultrahigh Molecular Weight Polyethylene via the Mobile Hexagonal Phase. *Macromolecules* **1998**, *31*, 5022–5031.
- (21) Ding, A. G.; Shenderova, A.; Schwendeman, S. P. Prediction of Microclimate PH in Poly(Lactic-Co-Glycolic Acid) Films. *J. Am. Chem. Soc.* **2006**, *128*, 5384–5390.
- (22) Sophocleous, A. M.; Desai, K.-G. H.; Mazzara, J. M.; Tong, L.; Cheng, J.-X.; Olsen, K. F.; Schwendeman, S. P. The Nature of Peptide Interactions with Acid End-Group PLGAs and Facile Aqueous-Based Microencapsulation of Therapeutic Peptides. *J. Controlled Release* **2013**, *172*, 662–670.
- (23) Yamamoto, M.; Takada, S.; Ogawa, Y. Sustained Release Microcapsule. U.S. Patent 5,330,767 A, 1994.
- (24) Hiroaki, O.; Masaki, Y.; Toshiro, H.; Yayoi, I.; Shigeru, K.; Yasuaki, O.; Hajime, T. Drug Delivery Using Biodegradable Microspheres. *J. Controlled Release* **1994**, *28*, 121–129.
- (25) Sandostatin LAR Depot (octreotide acetate for injectable suspension) [https://www.accessdata.fda.gov/drugsatfda\\_docs/label/1998/210081bl.pdf](https://www.accessdata.fda.gov/drugsatfda_docs/label/1998/210081bl.pdf).
- (26) Blasi, P.; D'Souza, S. S.; Selmin, F.; DeLuca, P. P. Plasticizing Effect of Water on Poly(Lactide-Co-Glycolide). *J. Controlled Release* **2005**, *108*, 1–9.
- (27) Desai, K.-G. H.; Schwendeman, S. P. Active Self-Healing Encapsulation of Vaccine Antigens in PLGA Microspheres. *J. Controlled Release* **2013**, *165*, 62–74.
- (28) Bouissou, C.; Rouse, J. J.; Price, R.; van der Walle, C. F. The Influence of Surfactant on PLGA Microsphere Glass Transition and Water Sorption: Remodeling the Surface Morphology to Attenuate the Burst Release. *Pharm. Res.* **2006**, *23*, 1295–1305.
- (29) Rastogi, S.; Kurelec, L.; Lemstra, P. J. Chain Mobility in Polymer Systems: On the Borderline between Solid and Melt. 2. Crystal Size Influence in Phase Transition and Sintering of Ultrahigh Molecular Weight Polyethylene via the Mobile Hexagonal Phase. *Macromolecules* **1998**, *31*, 5022–5031.
- (30) Grund, J.; Koerber, M.; Walther, M.; Bodmeier, R. The Effect of Polymer Properties on Direct Compression and Drug Release from Water-Insoluble Controlled Release Matrix Tablets. *Int. J. Pharm.* **2014**, *469*, 94–101.
- (31) Huang, J.; Mazzara, J. M.; Schwendeman, S. P.; Thouless, M. D. Self-Healing of Pores in PLGAs. *J. Controlled Release* **2015**, *206*, 20–29.
- (32) Beig, A.; Feng, L.; Walker, J.; Ackermann, R.; Hong, J.; Wang, Y.; Jiang, X.; Schwendeman, S. P. Development and Characterization of Composition-Equivalent Formulations to the Sandostatin LAR by the Solvent Evaporation Method. *AAPS Annual Meeting and Exposition 2018*: Washington, D.C., 2018.